

A Comparison between Ratio and Gradient Technique in Discriminating Cirrus Clouds from Tropospheric Aerosols over Water in MODIS Data

Asmala Ahmad

Faculty of Information and Communication Technology
Universiti Teknikal Malaysia Melaka (UTeM)
76100 Durian Tunggal, Melaka, Malaysia

Abd Rahman Mat Amin, Fadhli Ahmad

Faculty of Applied Science, Universiti Teknologi Mara (UiTM),
21080 Kuala Terengganu, Terengganu, Malaysia

Mustafa Mamat

Fakulti Informatik dan Komputeran, Universiti Sultan Zainal Abidin (UniSZA),
Kampus Tembila, 22200 Besut, Terengganu, Malaysia

Khiruddin Abdullah

School of Physics, Universiti Sains Malaysia (USM),
11800 Minden, Malaysia

Copyright © 2014 Asmala Ahmad et al. This is an open access article distributed under the Creative Commons Attribution License, which permits unrestricted use, distribution, and reproduction in any medium, provided the original work is properly cited.

Abstract

This study aims to compare between ratio technique (RT) and gradient technique (GT) to distinguish cirrus cloud from tropospheric aerosol over water in MODIS data. Both techniques make use of 1.375 μm and 1.240 μm band and are applied to five different scenes. The outcomes from both techniques are compared using an error matrix in which revealing that the GT has a very high agreement with RT in distinguishing cirrus cloud from tropospheric aerosol in MODIS data.

Keywords: Cirrus, Remote Sensing, MODIS, Aerosol, Gradient Technique

1 Introduction

Cloud is a source of error when retrieving aerosol and surface properties from remote sensing satellites [2], [7]. The presence of thin cirrus clouds in remote sensing data is conventionally difficult to detect in visible and IR atmospheric window regions because clouds are partially transparent in visible and near infrared wavelengths [5]. The Moderate Resolution Imaging Spectroradiometer (MODIS) is the key instrument of the Earth Observing System (EOS). It measures radiances using 36 bands ranging from visible to thermal infrared wavelengths with a spatial resolution of 250 m to 1 km [1], [9], [3]. The main objective of this study is to compare between ratio technique (RT) and gradient technique (GT) in distinguishing between tropospheric aerosols from cirrus cloud in MODIS data. The RT is based on the fact that the ratio of 1.375 μm and 1.240 μm of MODIS band is effective in separating the lower level dusts or aerosols from the upper level cirrus clouds [6]. The RT has also been incorporated into the operational MODIS aerosol algorithms for improved aerosol retrievals [6], [8]. On the other hand, the GT is based on the gradient of the line that connects the 1.375 μm and 1.240 μm band of the log–log graph of apparent reflectance against the MODIS wavelength [3].

2 Materials and Methods

The usefulness of the RT in separating between cirrus cloud and aerosols or dusts is due to the large contrast that exists between the 1.375 μm band and the 1.240 μm band. Dust pixels possess ratios of 0.1 or less, while the cirrus pixels possess ratio values greater than 0.3. In this study, the following RT algorithm was applied to the MODIS data acquired from different locations and dates:

$$\frac{\rho_{1.375}}{\rho_{1.240}} \quad (1)$$

where ρ_i is the reflectance recorded from a particular band i . For the GT, initially, eight MODIS bands (bands 1–7 and 26) were considered where the log–log graphs of the apparent reflectances from these bands against their wavelengths were plotted. Table 1 shows the MODIS bands and their wavelengths used in this study [9].

Table 1: MODIS bands and their wavelengths.

Band	Wavelength (μm)
1	0.659
2	0.865
3	0.470
4	0.555
5	1.240
6	1.640
7	2.130
26	1.375

Based on the graph, the gradient of the line that connects the 1.375 μm and 1.240 μm bands was chosen to discriminate cirrus cloud from aerosol in MODIS data. The variation in the gradient of this graph was highly correlated with the presence of aerosol and cirrus cloud over the study areas. The gradient can be expressed by:

$$\Delta m = \frac{\log_{10}(\rho_{1.375}) - \log_{10}(\rho_{1.240})}{\log_{10}(\lambda_{1.375}) - \log_{10}(\lambda_{1.240})} \quad (2)$$

where $\lambda_{1.375}$ and $\lambda_{1.240}$ are the central wavelengths and $\rho_{1.375}$ and $\rho_{1.240}$ are the apparent reflectances of 1.375 μm and 1.240 μm bands respectively. To avoid negative gradient values, we considered only gradient magnitudes by calculating the absolute gradient values. A gradient map was then constructed based on these values. It was found that the gradient of the lines varies according to the atmospheric composition. Cirrus area showed the lowest gradient compared to clear, hazy and dust influence area. In this study, pixels with a gradient value lower than -11.65 were discarded. In order to compare between the RT and GT, the error matrix technique was used. The accuracy assessment was conducted as follow. Firstly, the map for the RT and GT was developed based on the respective algorithms. In each map, the cirrus pixels were labelled as '1' while the cirrus clear pixels were labelled as '2'. Next, a comparison map was plotted, in which pixels by pixels comparison was performed. The pixels detected as cirrus by both algorithms were labelled as '11'. The pixels detected as cirrus by RT algorithm but detected as cirrus free by GT algorithm were labelled as '12'. The pixels detected as cirrus free by RT but as cirrus by GT were labelled as '21'. The pixels detected as cirrus free by RT and GT were labelled as '22'. The number of pixels in each class was then calculated. The error matrix was then constructed based on Table 2. The techniques were applied to the MODIS Terra satellite datasets that cover the following areas: China and the Korean peninsula at 0255 UTC 20 March 2001, Japan and Korean Peninsula at 0200 UTC 18 April 2006, Mediterranean Sea and north of Libya at 1130 UTC 23 January 2006, West Africa and Atlantic Ocean at 1155 UTC 2 March 2003 and Canada and nearby area at 1540 UTC 26 May 2007. Since the study meant for water areas, land area was masked out prior to performing the techniques.

Table 2: Error matrix.

	1	2	
1	N_{11}	N_{21}	$N_{11}+N_{21}$
2	N_{12}	N_{22}	$N_{12}+N_{22}$
	$N_{11}+N_{12}$	$N_{21}+N_{22}$	$N_{11}+N_{22}$

where,

N_{11} (Black) = number of pixels detected as cirrus by RT and GT.

N_{21} (Green) = number of pixels detected as cirrus by GT but as cirrus free by RT.

N_{12} (Red) = number of pixels detected as cirrus free by GT but as cirrus by RT.

N_{22} (Blue) = number of pixels detected as cirrus free by GT and RT.

The percentages of accuracy can be calculated based on the following expressions:

$$\text{User accuracy} = \frac{(N_{11})}{(N_{11} + N_{21})} \times 100\% \quad (3)$$

$$\text{User accuracy} = \frac{(N_{11})}{(N_{11} + N_{12})} \times 100\% \quad (4)$$

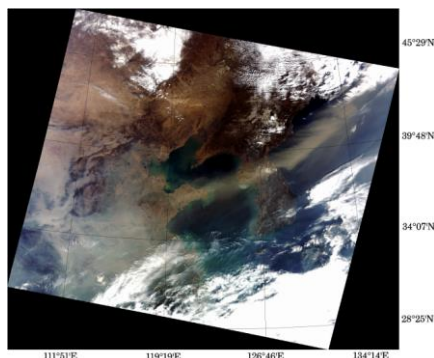
$$\text{Commission error} = \frac{(N_{21})}{(N_{11} + N_{21})} \times 100\% \quad (5)$$

$$\text{Omission error} = \frac{(N_{12})}{(N_{11} + N_{12})} \times 100\% \quad (6)$$

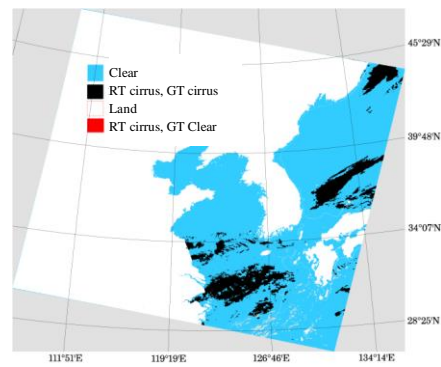
3 Results and Discussion

Figure 1 shows MODIS bands 1, 4 and 3 assigned to red, green and blue respectively, also known as the true colour combination, acquired over (a) China and the Korean peninsula at 0255 UTC on 20 March 2001, (c) Japan and Korean Peninsula at 0200 UTC on 18 April 2006, (e) Mediterranean Sea and Northern Libya at 1130 UTC on 23 January 2006, (g) West Africa and Atlantic Ocean at 1155 UTC on 2 March 2003, (i) Canada at 1540 UTC on 26 May 2007. Figure 1 (b), (d), (f), (h) and (j) are the corresponding comparison maps generated using the RT and GT algorithms. The MODIS scene in Figure 1(a) covers part of China Sea and Korean Peninsula where the presence of dust layer can be seen as brownish patches in the middle of the scene. In Figure 1(b), the blue regions represents the cirrus free or water area, while the white regions represents the land area. The pixels detected as cloud by RT and GT are represented by the black regions. Figure 1(c) covers Japan and Korean Peninsula showing brownish patches in the middle of the scene indicating the presence of a dust which is likely to be drifted from the Gobi Desert in China. In Figure 1(d) the cirrus cloud area (black region) seems to be the largest compared to the other dates. Figure 1(e) shows a scene acquired over the Mediterranean Sea near the north of Libya in which patches of cloud can be clearly seen on the top of the scene. Dust cloud can be seen on the top right of the scene. It is noticeable in Figure 1(f) that small portion of cirrus cloud represented by the black region can be seen near the coastal line and across the Persian Gulf. In Figure 1(g), it

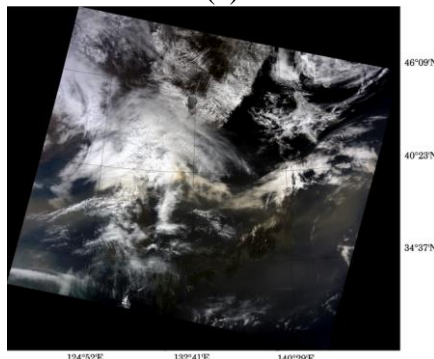
can be seen that dust plumes cover part of the Atlantic Ocean near the west of Africa (brownish patches). Patches of cloud are observed on the left of the scene. As seen in Figure 1(h), not much cirrus cloud can be detected by the algorithms. The scene in Figure 1(i) covers part of Canada where patches of dust can be clearly observed in the middle of the scene. In Figure 6(j), the presence of cirrus clouds is indicated by the black regions in the middle and bottom right of the map.



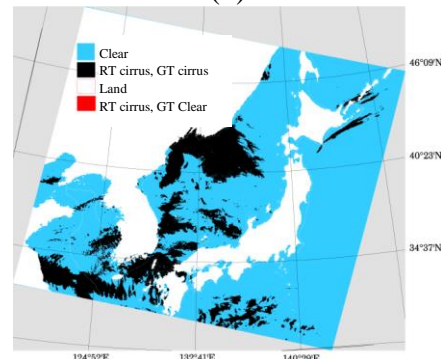
(a)



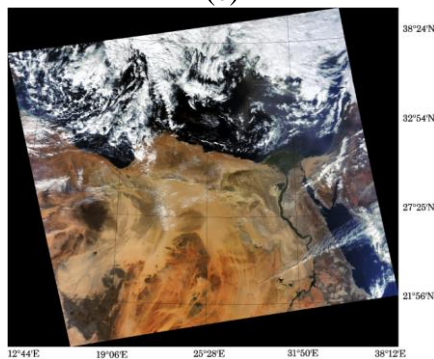
(b)



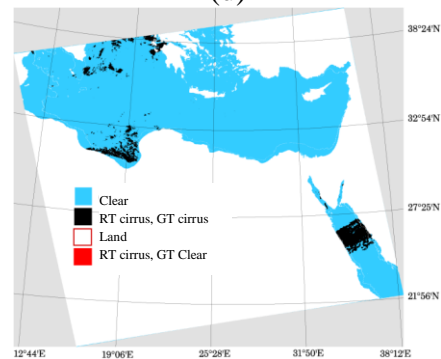
(c)



(d)



(e)



(f)

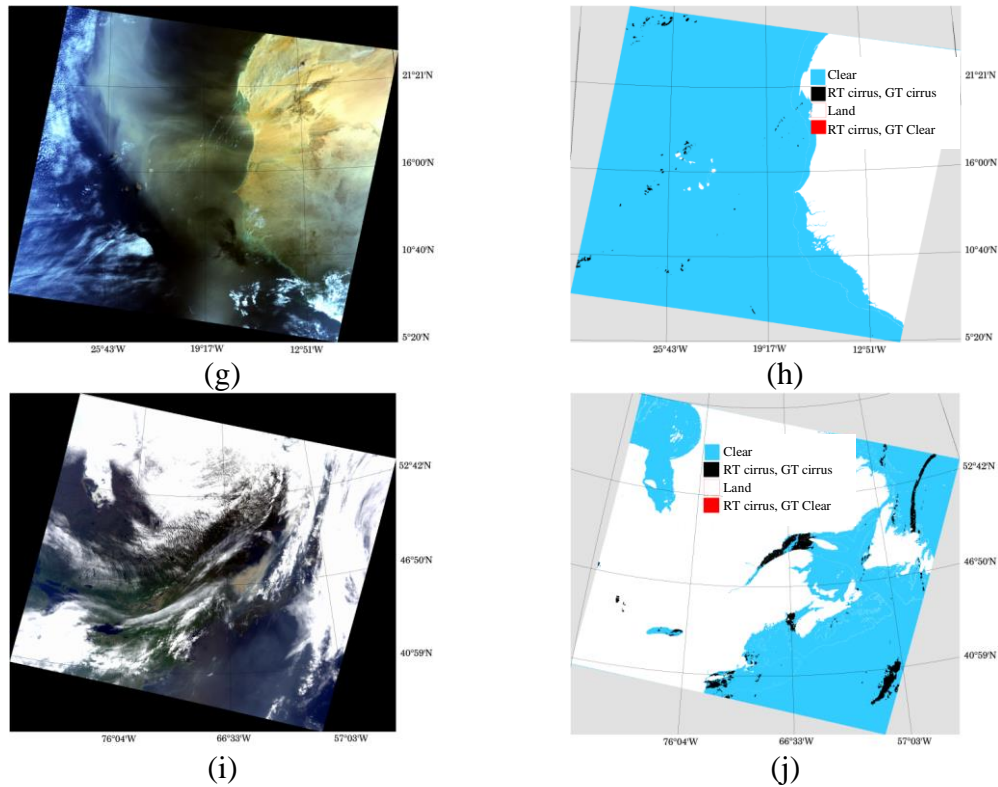


Figure 1: MODIS bands 1, 4 and 3 assigned to red, green and blue of a MODIS acquired over (a) China and the Korean peninsula at 0255 UTC on 20 March 2001, (c) Japan and Korean Peninsula at 0200 UTC on 18 April 2006, (e) Mediterranean Sea and north of Libya at 1130 UTC on 23 January 2006, (g) West Africa and Atlantic Ocean at 1155 UTC on 2 March 2003, (i) Canada and nearby area at 1540 UTC on 26 May 2007. (b), (d), (f), (h) and (j) are the corresponding comparison maps of the RT and GT.

The outcomes of the gradient and ratio technique were compared by making use of a confusion matrix (Table 3). In overall, the user accuracy and producer accuracy is given by 100% and 99.99% respectively. The commission percentage is given by 0% because no pixels are classified as cirrus by GT but clear by RT in the N_{21} column. On the other hand, some pixels are detected as cirrus by RT but clear by GT as shown in the N_{12} column producing the overall percentage of omission pixels is 0.01%. However, these pixels are not visible in the maps due to the very small amount.

4 Conclusions

A comparison study between RT and GT has been carried out on five different locations and dates of MODIS data. The RT is based on the ratio of MODIS 1.375

μm and $1.240 \mu\text{m}$ band, while the GT algorithm is based on the gradient of the line connecting the $1.375 \mu\text{m}$ and $1.240 \mu\text{m}$ bands of a log–log graph of apparent reflectance versus MODIS wavelengths. Comparison analysis using an error matrix shows that GT and RT algorithm have a very high agreement in distinguishing cirrus cloud from tropospheric aerosol in MODIS data.

Table 3: Accuracy assessment results.

Location	Ratio Technique (RT)				
	Class	Cirrus	Clear	Commission Error (%)	Producer Accuracy (%)
China Sea	Cirrus	216417	0	0	100
	Clear	13	1485526	0	100
	Omission Error (%)	0.01	0		
	User Accuracy (%)	99.99	100		
Japan and Korean Peninsula	Cirrus	537989	0	0	100
	Clear	27	2306437	0	100
	Omission Error (%)	0.01	0		
	User Accuracy (%)	99.99	100		
Mediterranean Sea	Cirrus	77908	0	0	100
	Clear	7	1502361	0	100
	Omission Error (%)	0.01	0		
	User Accuracy (%)	99.99	100		
Atlantic Ocean	Cirrus	10628	0	0	100
	Clear	0	3269947	0	100
	Omission Error (%)	0	0		
	User Accuracy (%)	100	100		
Canada	Cirrus	90617	0	0	100
	Clear	8	1806637	0	100
	Omission Error (%)	0.01	0		
	User Accuracy (%)	99.99	100		

Acknowledgment

We would like to thank UiTM Kuala Terengganu, UMT, USM and UTeM for the support and encouragement. This project is jointly funded by the UiTM Excellent Grant (600-UiTMKD (PJI/RM U/ST/DANA 5/2/1-08/20/2012)) and UTeM Short

Term Grant (PJP/2013/FTMK(2B)/S01104). Our appreciation also goes to the MODIS team for the valuable data provided.

References

- [1] A. Ahmad and S. Quegan, Multitemporal Cloud Detection and Masking Using MODIS Data, *Applied Mathematical Sciences*, 8(7) (2014), 345–353.
- [2] A. Ahmad, M.K.A. Ghani, S. Razali, H. Sakidin and N.M. Hashim, Haze Reduction from Remotely Sensed Data, *Applied Mathematical Sciences*, 8(36) (2014), 1755–1762.
- [3] A. Asmala, A.R.M. Amin, A. Fadhli, M. Mustafa and A. Khiruddin, Euphotic Depth Zone Variation in Peninsular Malaysia Maritime. *Applied Mathematical Sciences*, 8(68), (2014). 3375–3383.
- [4] AR.M. Amin, K. Abdullah and M. Rivaie, Discriminating cirrus cloud from MODIS imagery over oceans utilizing gradient technique, 2011 IEEE Colloquium on Humanities, Science and Engineering (CHUSER), (2011), 513–518.
- [5] B.C. Gao and R.R. Li, The spatial and temporal variations of high clouds based on the MODIS 1.375 micron channel measurements, *IEEE International Geoscience and Remote Sensing Symposium, IGARSS 2008*, (2008), 582–585.
- [6] B.C. Gao, Y. Kaufman, D. Tanre, and R.R. Li, Distinguishing tropospheric aerosols from thin cirrus clouds for improved aerosol retrievals using the ratio of 1.38 μm and 1.24 μm channels, *Geophys. Res. Lett.*, 29(999918), 1890, (2002).
- [7] M.I. Mishchenko, I.V. Geogdzhayev, B. Cairns, W.B. Rossow and A.A. Lacis, Aerosol retrievals over the ocean by use of channels 1 and 2 AVHRR data: sensitivity analysis and preliminary results, *Applied Optics*, 38 (1999), 7325–7341.
- [8] R.C. Levy, L.A. Remer, D. Tanre, S. Matoo and Y.J. Kaufman, Algorithm for Remote Sensing of Tropospheric Aerosol From MODIS: Collection 005 and 0.51, [online] Available: <http://modis-atmos.gsfc.nasa.gov>, (2009).
- [9] S.A. Ackerman, K.I. Strabala, W.P. Menzel, R. Frey, C. Moeller, L. Gumley, B.A. Baum, S.W. Seaman and H. Zhang, Discriminating clear-sky from cloud with MODIS algorithm theoretical basis document (MOD35). ATBD-MOD-06, Version 5.0, (2010), NASA, Greenbelt, MD.

Received: August 5, 2014